PHYSICAL REVIEW B VOLUME 21, NUMBER 8 15 APRIL 1980

"Thomas-Fermi-pseudopotential" approach for calculating the static properties of simple metals

James R. Chelikowsky
Department of Physics, Institute of Theoretical Science, University of Oregon, Eugene, Oregon 97403
(Received 18 October 1979)

A completely local-density energy-functional pseudopotential study is performed to analyze the static properties of several simple metals. The great advantages of calculating the electronic structure of solids with local-density energy-functional approaches, or "Thomas-Fermi" approaches, are that these approaches, unlike fully quantum-mechanical treatments, possess the attributes of simplicity, flexibility, and physical immediacy. The local-energy-density functional can yield accurate static properties provided we employ "hard-core" pseudopotentials which have been derived from atomic charge densities. Moreover, our approach allows a real-space decomposition of the various energy contributions to cohesion.

I. INTRODUCTION

While the Thomas-Fermi method[1] and the closely related energy-density-functional (EDF) method[2-4] have had a long and venerable history in the description of the electronic structure of solids, they have been supplanted in modern discussions by fully quantum-mechanical methods. The reasons for this are clear: EDF methods, while yielding qualitatively correct and, in some cases, semiquantitative descriptions of electronic properties, are just too crude in comparison with the more sophisticated quantum-mechanical procedures available. The major problems associated with local EDF approaches involve the absence of any phase correlations. Thomas-Fermi procedures consider the total electronic energy of a system to be a functional of the charge density; no wave functions are involved. Consequently Thomas-Fermi approaches do not contain quantum interference effects nor do they properly treat orbital-hybridization (directional-bonding) effects. Moreover, the shell structure of the "Thomas-Fermi" atom is absent.[5] These inherent flaws of EDF approaches mean that any calculated atomic properties can vary only monotonically with atomic number. In addition EDF approaches do not lead to cohesion in molecules or solids[6-8] unless gradient or higher-order corrections are made to the usual Thomas-Fermi kinetic energy expression. To date, the exact nature of the gradient terms has not been clearly elucidated; this problem remains an area of continuing examination.[9-12] Finally, EDF approaches are restricted only to considerations of ground-state properties.

The deficiencies of EDF approaches might appear insurmountable; however, EDF approaches do possess some redeeming features. For example, they are simple and flexible. Moreover, they have the advantage of physical immediacy, e.g., no band-structure calculations, no density-of-states calculations, etc. are needed to determine the static properties of a metal. In addition the EDF approach is easy to interpret and can be used to relate microscopic quantities to thermochemical properties. Therefore, if some of the major deficiencies of EDF approaches could be removed these approaches would prove to be very powerful techniques in obtaining an understanding of the electronic properties of solids.

In the present work we hope to illustrate how some of the deficiencies of EDF approaches can be eliminated. Specifically, we will demonstrate that an EDF approach which employs "hard-core" pseudopotentials[13,14] derived from atomic charge densities is capable of yielding quantitative results for the static properties of simple metals. As a case study we will examine several simple metals: Li, Na, K, Rb, Cs, Mg, Ca, and Al.

The possibility of using a pseudopotential constructed within the EDF approach has not been investigated in past studies, but the coupling of an EDF approach with pseudopotential formalism has numerous advantages.[15] Our pseudopotential construction is based on the "true" valence charge density as calculated via a local-density exchange-correlation formalism. We require that the pseudopotential reproduce the true density away from the core region. This requirement means that our pseudopotential implicitly contains the shell structure of the atom. Consequently, our calculated atomic properties within an EDF-pseudopotential framework need not vary in a monotonic fashion with atomic number. In addition we will establish a criterion for obtaining an accurate local expression for the kinetic energy within this framework. Second, our procedure has several practical advantages over the more conventional approaches. For example, our pseudopotentials involve no parameters adjusted to experimental data; thus, they are of a "first-principles" nature. The calculations involve computing

the differences between the electronic energy of the valence electrons of the atom and the conduction electrons of the metal. This energy difference is significant compared to the individual energies involved, and the high numerical precision required in other techniques[16-18] is not required in our approach. As a consequence, calculations for heavy metals using this method are easily performed. Moreover, the use of pseudopotentials means that the effective potential is weak; this allows us to employ simple trial functions for the density and this implies an EDF approach might be very accurate. Finally, with respect to these pseudopotential techniques, we note that only the valence electrons are retained in our method. This allows us to extract the valence electron contributions to cohesion without having to carry the essentially passive core states.[16-18]

Our interest in obtaining a workable energy-density-functional approach and applying the approach to metals has been stimulated by the recent progress in developing techniques, both *ab initio* and empirical, for predicting and understanding the properties of intermetallic compounds and alloys. While it is possible, using currently available methods, to compute from first principles cohesive properties of metals and ordered alloys, at present such an approach does not appear to be a feasible mechanism for developing a global picture. *Ab initio* calculations[16-18] are difficult, employ extensive computing facilities, and lack the required flexibility to achieve this goal. The situation has motivated, over the last few years, the creation of several empirical or semiempirical schemes.[19-26] While many of these schemes are quite successful, a major problem with most of them is that they do not provide us with a definitive microscopic interpretation of metallic properties. One long-range goal of the present effort is to develop a scheme which can be closely related to a microscopic interpretation and yet be amenable to studying and predicting accurate intermetallic properties.

II. ENERGY-DENSITY-FUNCTIONAL PSEUDOPOTENTIAL

In this section we will define an ionic pseudopotential which, when screened in a self-consistent fashion within the EDF approach, will yield an accurate charge density in a region away from the core region. Our starting point is to write the total electronic energy E as a function of the valence charge density. In atomic units (a.u.) we have

$$E(n) = C_0 \int n^{5/3}\, d\tau + C_1 \int \frac{(\nabla n)^2}{n}\, d\tau + \int n V_p^i\, d\tau + \tfrac{1}{2} \int n V_H\, d\tau + E_{xc}(n)\,, \qquad (1)$$

where C_0 and C_1 are constants, V_p^i is the ionic pseudopotential which represents the effective potential of the nucleus plus core electrons, V_H is the electrostatic potential from Poisson's equation, and $E_{xc}(n)$ is an exchange-correlation local-density expression as in the work of Gunnarsson *et al.*[27] The first two terms in Eq. (1) are kinetic energy terms. The choice of coefficients C_0 and C_1 will be discussed in Sec. III.

Once we have written the total electronic energies down as in Eq. (1), we may take the functional derivative of $E(n)$ with respect to δn under the constraint that n be normalized. The result is an equation for n:

$$-4C_1 \frac{\nabla^2 n^{1/2}}{n^{1/2}} + \tfrac{5}{3} C_0 n^{2/3} + V_p^i + V_H + \mu_{xc} + V_0 = 0\,, \qquad (2)$$

where μ_{xc} is the functional derivative[27] of $E_{xc}(n)$ and V_0 is a Lagrangian multiplier to insure charge conservation (it corresponds to the Fermi level in Thomas-Fermi theory). The point to note here is that we may invert Eq. (2) to obtain an equation for V_p^i:

$$V_p^i = -V_0 - V_H - \mu_{xc} + 4C_1 \frac{\nabla^2 n^{1/2}}{n^{1/2}} - \tfrac{5}{3} C_0 n^{2/3}\,. \qquad (3)$$

If we are *given* a valence charge density n, we may then use Eq. (2) to find the potential which will reproduce this density.

To define V_p^i we will consider a pseudocharge density designed to be a smooth, nodeless function which agrees exactly with the true atomic valence charge density away from the core region. This is illustrated in Figs. 1 and 2. We will consider only the atomic charge density and assume that the ionic pseudopotential determined by atomic density consideration is transferable from the atom to the solid. This assumption is equivalent to the "frozen-core" approximation. This approximation has recently been discussed by Moriarty,[28] and he has shown it to be valid even with respect to structural energy differences.

One additional comment should be made with respect to Eq. (3). Namely, how unique is the potential in Eq. (3)? If we demand that our pseudocharge density agree with the true valence density away from the core region, i.e., beyond the outermost node of the valence density, then this part of the potential is uniquely determined. The core region is not uniquely fixed by this procedure; however, if we demand that the total pseudocharge be normalized, then the amount of charge in this region is restricted to be small, e.g., less than ~5% of the total. This means that this region cannot be of significance with respect to the static properties of a metal. First the charge in this region is small, and second any errors in this region will

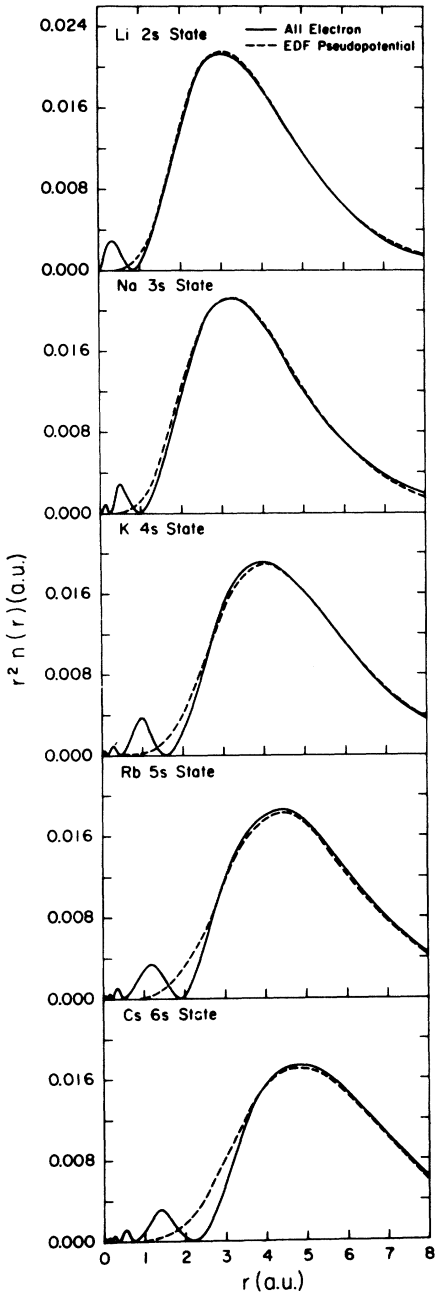

FIG. 1. Radial distribution functions for the alkali metals. The pseudocharge density is of the form given by Eq. (8). This pseudocharge density is used to define the energy-density-functional pseudopotential as in Eq. (3).

be canceled when we take energy differences between the atom and metal.

III. LOCAL EXPRESSIONS FOR THE KINETIC ENERGY

Local expansions of the kinetic energy have recently been studied by several groups, e.g., Parr

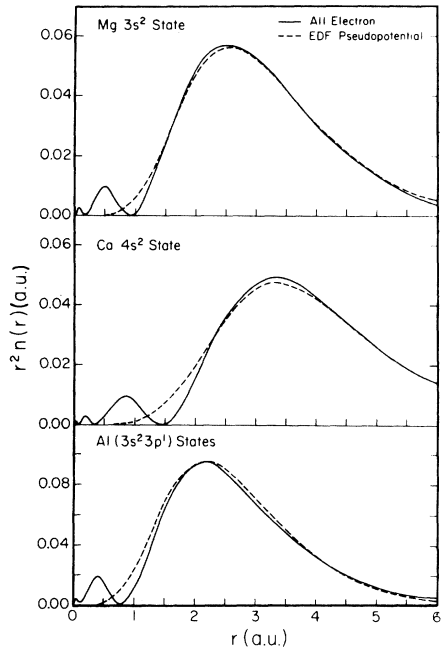

FIG. 2. Radial distribution functions for Mg, Ca, and Al. In Al note that we consider the total valence density. The form of the pseudocharge density is given by Eq. (8). We use this pseudocharge density to define the energy-density-functional pseudopotential from Eq. (3).

et al.,[10] Alonso and Girifalco,[11] Tal and Bader,[12] and Oliver and Perdew.[9] Most of these studies have concentrated on either assessing the accuracy of local kinetic energy expansions or including nonlocal corrections to the kinetic energy expressions. Here we will concentrate on providing a practical, realistic local expression for the kinetic energy. We shall invoke one parameter in our discussion. Our single parameter will be fixed by theoretical considerations alone and not by experimental data.

In Eq. (1) we had two coefficients C_0 and C_1 entering our kinetic energy experession. C_0 is the usual Thomas-Fermi coefficient: $C_0=\frac{3}{10}(3\pi^2)^{2/3}$. The value to be used for the coefficient C_1 is not so clear. The value of $C_1=\frac{1}{8}$ was originally suggested by Von Weizsacker.[29] We note that more recent derivations[2,30] using different limiting conditions on the charge fluctuations have produced a value of $C_1=\frac{1}{72}$. For atomic systems, if Hartree-Fock charge densities are used, the coefficient of $C_1=\frac{1}{72}$ seems to reproduce quite accurately the true Hartree-Fock kinetic energy.[5,10] Our calculations, however, indicate that $C_1=\frac{1}{72}$ will not yield accurate kinetic energies for a pseudocharge density. There are several reasons for this situation. First, we have eliminated core states from any consideration. In atoms the core states dominate

the kinetic energy, and while the coefficient $C_1 = \frac{1}{72}$ may be appropriate for core state configurations we have no reason to believe it is appropriate for valence states alone. Second, we do not have the true all-electron charge density in our calculation, but rather pseudodensities which possess no nodal structure and cannot be expected to yield all-electron values for the kinetic energy. Third, our pseudopotential already contains "kinetic energy" contributions from the requirement that the valence states be orthogonal to core states.[31]

To fix a realistic coefficient for our kinetic energy expansion, we proceed as follows. We consider the atomic pseudocharge densities. We note that our atomic pseudocharge densities are nodeless and, therefore, we may write an equivalent pseudo-wave function as $\psi_p = \sqrt{n_p}$. To be formally correct we consider only the *angularly* averaged densities. If we have more than one state present, we may define $\psi_p^l = \sqrt{n_p^l}$ for each l component of the density. In this case, the correct *quantum-mechanical* kinetic energy is given by

$$T_{QM} = \tfrac{1}{8} \sum_l \int \frac{(\nabla n_p^l)^2}{n_p^l}\, d\tau + \sum_l \int \frac{l(l+1)}{2r^2}\, n_p^l\, d\tau \,. \tag{4}$$

In this fashion we can calculate what the actual quantum-mechanical kinetic energy should be for our pseudocharge densities. We then fix C_1 so that

$$T_{\rm QM} = T_{\rm EDF} = C_0 \int n_p^{5/3}\, d\tau + C_1 \int \frac{(\nabla n_p)^2}{n_p}\, d\tau \,, \tag{5}$$

where $n_p = \sum_l n_p^l$ is the total valence pseudocharge density. By demanding $T_{\rm QM} = T_{\rm EDF}$ we guarantee that our atomic calculation within the EDF framework will yield *exactly* the quantum-mechanical kinetic energy. We note that our procedure is similar to the X_α technique of fixing the exchange-correlation coefficient α. In the X_α procedure developed by Schwarz,[32] the parameter α is fixed to reproduce exactly the Hartree-Fock total energy of the atom. The parameter α so fixed by the atomic calculation is then transferred to molecular or solid state calculations. We shall make a similar assumption here, i.e., that C_1 is transferable from the atom to the metal. This is, perhaps, a stronger assumption but, as we shall see, the gradient term for the metal is quite small compared to the leading Thomas-Fermi term. As a consequence any error in the metal because of our choice of C_1 should be small. One other advantage in fixing C_1 via Eq. (5) is that we may effectively absorb higher-order terms in a kinetic energy expansion into our coefficient C_1. These higher-order terms are not important in the metal; so, by fixing the atom to the "correct" kinetic energy behavior, we eliminate problems concerned with gradient corrections beyond the leading term.

IV. METHODS OF CALCULATION

Our first task in evaluating the static properties of metals is to obtain accurate ionic pseudopotentials within the EDF scheme as specified in Eq. (3). To accomplish this task we need accurate pseudocharge densities. We obtain these densities by considering the all-electron solution of Hartree-Fock equations for the free atom[33] within a local-density exchange-correlation approximation. We solve for the atomic eigenvalues and eigenfunctions with a potential of the form:

$$V = -\frac{z}{r} + \int \frac{n_t}{|\vec{r} - \vec{r}'|}\, d\tau' + \mu_{\rm xc}(n_t) \,, \tag{6}$$

where the exchange-correlation potentials $\mu_{\rm xc}$, is of the following form:[27,34]

$$\mu_{\rm xc} = -[1 + 0.0545 \ln(1 + 11.4/r_s)]/\pi\alpha r_s \,, \tag{7}$$

with $\alpha = (4/9\pi)^{1/3}$ and $\frac{4}{3}\pi r_s^3 = 1/n_t$. n_t is the *total* charge density for the atom. The local-density approximation to exchange and correlation appears to yield quite accurate ground-state properties.[18] It does not yield accurate excited or dynamic properties, but we will not be concerned with such matters in the present work. One point which we should mention is that in Eq. (1) we have written $\mu_{\rm xc}(n_p)$ instead of a more proper $\mu_{\rm xc}(n_t) - \mu_{\rm xc}(n_{\rm core})$; i.e., we have neglected valence-core exchange effects. This approximation appears to be quite valid and has recently been discussed by Moriarty.[28]

In choosing a pseudocharge density, our goal is to reproduce accurately the all-electron charge density away from the core region. We choose the following analytic function and fit the parameters a_i to the all-electron density beyond the outermost node.

$$n_p(r) = [1 - \exp(-a_0 r^2)] \times [a_1 r^2 \exp(-a_2 r) + a_3 r^3 \exp(-a_4 r)] \,. \tag{8}$$

Our resulting pseudocharge density and calculated all-electron charge densities for the valence electrons are illustrated in Figs. 1 and 2. We display the radial distribution functions which are a reliable means of assessing the accuracy of any fit.

The prefactor in Eq. (8) is essential in obtaining an accurate fit. If we wish to have accurate densities away from the core region *and* to have properly normalized densities, then the latter requirement demands that charge be excluded from the core region. We must include the damping

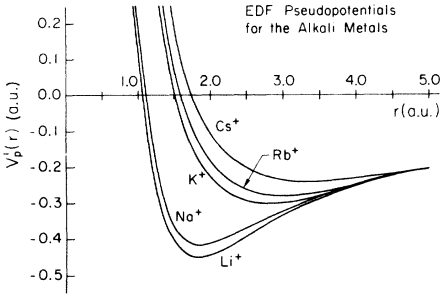

FIG. 3. Energy-density-functional ionic pseudopotentials for the alkali metals [Eq. (3)]. Note the strong $(1/r^2)$ divergence in the core region. This divergence appears to be an important aspect of EDF pseudopotentials (see text).

prefactor to accomplish this. In Table I we list the coefficients a_i. While Eq. (8) yields a credible fit to the all electron densities for the elements we wish to examine, the coefficients are not uniquely determined. Therefore, we do not attach any physical interpreation to the coefficients a_i.

With the densities so fixed we need to evaluate our kinetic energy expansion parameter C_1 before we can construct the ionic pseudopotentials. We calculate C_1 via Eq. (5). For Al this requires some care. We calculate the s- and p-electron kinetic energies separately via Eq. (4). However, in Eq. (5) we must employ the total density. We use the same expressions for the s- and p-charge densities as for the total density in Al. This is convenient, but it does result in some loss of accuracy. Unfortunately, C_1 is fairly sensitive to the tails of the charge-density distributions. Thus we used a very accurate numerical scheme to perform the integrations. We feel that our C_1 parameters are accurate to within a few percent, and this precision appears to yield static properties with a similar accuracy. The C_1 parameters are presented in Table II. The reader will note that they all fall between the two limiting cases of $C_1 = \frac{1}{8}$ for rapidly varying charge fluctuations and $C_1 = \frac{1}{72}$ for slowly varying charge fluctuations.

TABLE I. Parameters in a.u. for the atomic pseudocharge density as given in Eq. (8). The atomic pseudocharge density will accurately reproduce, away from the core region, the valence charge density as calculated by Hartree-Fock local-density exchange-correlation techniques for the all-electron atom. A comparison of the pseudocharge density and the true charge density is presented in Figs. 1 and 2.

Metal	a_0	a_1	a_2	a_3	a_4
Li	0.606 5	0.006 74	1.244	0.006 17	1.732
Na	0.898 8	0.001 02	1.720	0.008 149	1.521
K	0.149 3	0.000 079 8	0.747	0.004 32	1.352
Rb	0.106 6	0.000 012 1	0.547	0.003 829	1.304
Cs	0.064 35	0.000 000 9	1.578	0.002 739	1.197
Mg	0.075 47	0.079 0	1.640	1.127	2.806
Ca	0.239 9	0.002 10	1.260	0.023 48	1.601
Al(tot)	1.999	0.000 055	6.375	0.271 3	2.264
Al(3s)	0.612 5	0.002 85	1.196	0.031 78	2.024
Al(3p)	0.756 6	0.001 38	1.180	0.350 5	2.528

TABLE II. Coefficients for the gradient expansion term of the kinetic energy as defined by Eq. (5).

Metal	C_1	Metal	C_1
Li	0.067	Cs	0.073
Na	0.068	Mg	0.036
K	0.071	Ca	0.041
Rb	0.072	Al	0.037

From Eq. (3) we may now evaluate the ionic pseudopotentials; the potentials are displayed in Figs. 3 and 4. For small r we note that the potentials diverge quite strongly. This divergence is directly related to the requirement that the charge density vanish as $r \to 0$. While we need not require the pseudocharge density to vanish identically as $r \to 0$, we are required to normalize the density and, as indicated earlier, this requirement results in a minimal amount of charge within the ion core. Formally, if $\psi_p \sim r^m$ for small r, then our ionic pseudopotential will diverge as $1/r^2$ for small r for any $m > 0$.

Recently the $1/r^2$ divergence of hard-core pseudopotentials has been discussed in detail by several groups.[13,14] In particular, it appears that ionic radii based on the "classical" turning point[13] of these potentials provide very powerful structural indices. It is worth speculating that the $1/r^2$ divergence or hard-core aspect of pseudopotentials may be an essential feature of the potential for obtaining proper structural energy trends, lattice constants, phonon spectra, etc. In this respect it appears that the gradient term in the ki-

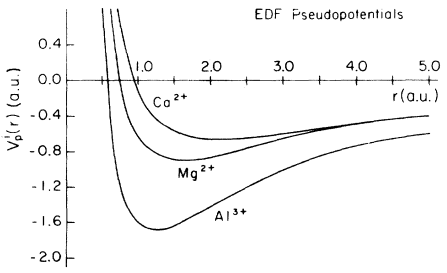

FIG. 4. Energy-density-functional ionic pseudopotentials as defined by Eq. (3) for Mg, Ca, and Al.

netic energy is an important feature of the potential defined via Eq. (3). Without the gradient term, we would not obtain a repulsive potential, i.e., the $1/r^2$ divergent term, or for that matter, cohesion in solids.

Once the ionic pseudopotential has been established from Eq. (3) we may calculate the total energy of the atom via Eq. (1). Next we solve for the energy per atom of the metal by employing spherical boundary conditions as originally suggested by Wigner and Seitz.[35] We replace the Wigner-Seitz polyhedral unit cell by a sphere of equal volume and we demand that the derivative of the metallic charge density vanish at the cell boundary: $(dn/dr)_{R_s}=0$, where R_s is the sphere radius.

To determine the metallic charge density and the corresponding metallic energy we write a trial density n_m of the form:

$$n_m(r)=\sum_{p=1}^{N} b_p \sin^2\left(\frac{p\pi}{R_s}r\right)\exp[c_p(r-R_s)^2] \qquad (9)$$

and minimize the energy with respect to varying the parameters (b_p, c_p). This expression appears to be very rapidly convergent and has the advantage of automatically having a vanishing slope at the spherical cell boundary. Tests with varying N indicate that even with $N=2$ the energy is converged to within ~0.01 eV. Our isotropic expression for the metallic density is satisfactory for close-packed and body-centered-cubic metals but for open structures it must be refined to include any angular dependence.

We calculate the metallic energy for several values of R_s. By locating the minimum energy as a function of R_s we determine the equilibrium sphere size R_s^0. Also by determining the curvature of $E_m(R_s)$ we can establish the compressibility or bulk modulus of the solid. Within this framework we can calculate four quantities: the electronic energy of the valence electrons of the free atom, the cohesive energy, equilibrium sphere size or atomic volume, and the bulk modulus.

Before discussing our results for the simple metals we have examined, we need to discuss a correction to the atom energy which is significant for atoms with open shells, i.e., spin-polarization effects.[18,27] These effects have been demonstrated by Gunnarsson *et al.*[27] to be essential in obtaining accurate cohesive energies. Fortunately, the spin-polarization corrections are easy to perform for nonmagnetic solids; we need only correct the atomic energies. For the cohesive energy we write

$$E_{\text{cohesion}}=E_{\text{metal}}-E_{\text{atom}}-\Delta E_{\text{sp}}\ , \qquad (10)$$

where ΔE_{sp} is the spin-polarization correction to the atomic energy, E_{metal} and E_{atom} are calculated from Eq. (1). ΔE_{sp} is calculated as in the work of Gunnarsson *et al.*[27] with the only difference being that we employ perturbation theory. The use of perturbation theory is quite accurate since ΔE_{sp} is typically less than 0.1% of the total atomic energy for the elements considered here.

We write ΔE_{sp} as

$$\Delta E_{\text{sp}}=\int [E^{\text{xc}}(r_s,\xi)-E^{\text{xc}}(r_s,0)]n\,d\tau\ , \qquad (11)$$

where $\xi=(n_\uparrow-n_\downarrow)/n_t$. Here we approximate $n_\uparrow$ and $n_\downarrow$ by the unpolarized density, e.g., $n_\uparrow-n_\downarrow=n_{3s}$ for Na. For $E^{\text{xc}}(r_s,\xi)-E^{\text{xc}}(r_s,0)$ we have from Ref. 27:

$$E^{\text{xc}}(r_s,\xi)-E^{\text{xc}}(r_s,0)$$
$$=\{(2^{1/3}-1)E_p^x-C_F[(1+X_F^3)\ln(1+1/X_F)+\tfrac{1}{2}X_F-X_F^2-\tfrac{1}{3}]+C_p[(1+X_p^3)\ln(1+1/X_p)+\tfrac{1}{2}X_p-X_p^2-\tfrac{1}{2}]\}f(\xi)\ , \qquad (12)$$

where $f(\xi)=[(1+\xi)^{4/3}-(1-\xi)^{4/3}-2]/(2^{4/3}-2)$, $E_p^x=-3/(4\pi\alpha r_s)$, $C_F=0.0203$, $C_p=0.0333$, $X_F=r_s/15.9$, and $X_p=r_s/11.4$.

Finally, with respect to Eq. (10), we have neglected the zero-point energy of the lattice vibrations. This energy is negligible in most cases (and certainly less than the uncertainties existing in the present calculations).[18]

V. RESULTS AND DISCUSSION

In Table III we compile our calculated binding energies for the valence electrons of the free atoms. We compare our calculations to experiment and to an all-electron calculation from Moriarty[28] for the valence electrons energy. We have corrected his values to include spin polarization for the open-shell atoms and indicate the corrections made. The all-electron binding energies for the valence electrons are accurate to 1.7% while our EDF pseudopotential achieves an overall accuracy of about 2.3%. The pseudopotential results appear to be slightly less accurate for the polyvalent metals, especially compared to the all-electron results.[28] However, we do not view this

as a significant problem as only the energy differences enter the cohesive energy in Eq. (10). Provided we make similar errors for both the metal and the atom, our cohesive-energy accuracy can be much better than the absolute errors listed in Table III.

In Tables IV–VI we present the results of our calculations for the cohesive energy, equilibrium radius, and bulk modulus for each metal. We compare our results to experiment and to what we believe are the best *ab initio* calculations for the static properties of these metals. These latter calculations have been performed by Moruzzi *et al.*,[17,18] and they will serve as our standard of comparison. The only input information into the Moruzzi *et al.*[18] calculation is the atomic number and the crystal structure of the metal.

With respect to the cohesive energies in Table IV, our overall accuracy appears to be competitive with the results of Moruzzi *et al.*[18] However, there are some interesting differences. For example, while the calculations of Moruzzi *et al.*[18] are exceedingly accurate for the light alkali metals, they do not appear to be equally accurate for the heavy alkalis, e.g., Rb or the polyvalent metals. The reasons for this trend are not transparent, and they do not appear to be present in our calculations. On the other hand, our calculations are deficient in that we do not properly include l-dependent or nonlocal effects. This deficiency becomes evident in Li and Ca. For example, Li and Na have almost identical valence charge densities away from the ion core (Fig. 1); however, Li has a cohesive energy which is approximately 40% larger than Na. We conclude that the significant differences between Li and Na metals must arise from excited-state admixtures into the metallic density as we pass from the atom to the metal. We do not include in our work the possibility of unoccupied states of the atom admixing into our metallic ground-state properties. In Ca a similar effect appears possible. In the alkali-earth column of the Periodic Table we do not observe a monotonic decrease in binding as we do in the alkali metals. Experimentally, Mg has a smaller cohesive energy than Ca; we observe in our calculations the opposite effect. We suspect that what is missing in our calculation is the absence of any d-state mixing which probably occurs in the metallic state of Ca. This seems reasonable since Ca precedes the first transition metal Sc and has an unoccupied d state which lies quite close to the ground state of the free atom. Moreover, the im-

TABLE IV. Cohensive energies as calculated from an energy-density-functional pseudopotential (EDFP) for several simple metals. The experimental cohesive energies are taken from Lewis *et al.* (Ref. 37). The all-electron values are from the calculation of Moruzzi *et al.* (Ref. 18). All energies are in eV.

Metal	Experiment	Theory all-electron	EDFP
Li	1.65	1.65	1.41
Na	1.13	1.12	1.22
K	0.94	0.90	1.07
Rb	0.86	0.64	0.99
Cs	0.83		0.94
Mg	1.53	1.69	1.88
Ca	1.83	2.24	1.72
Al	3.34	3.84	2.98
Accuracy		11.5%	12.2%

TABLE III. Valence-electron binding energy for several simple metals as calculated from an enery-density-functional pseudopotential. Also presented are the experimental values from Ref. 36 and the all electron calculations from Moriarty (Ref. 28). Spin polarization corrections are indicated in parentheses for the open-shell atoms (see text). All energies are in eV.

Metal	Experiment	All-electron	EDF pseudopotential
Li	5.39	5.56	5.50 (0.33)
Na	5.14	5.37	5.29 (0.29)
K	4.34	4.50	4.36 (0.22)
Rb	4.18	4.20	4.21 (0.20)
Cs	3.89	3.90	3.82 (0.17)
Mg	22.68	22.82	21.27
Ca	17.98	18.06	17.49
Al	53.25	53.30	54.26 (0.18)
Accuracy		1.7%	2.3%

TABLE V. Equilibrium sphere radii as calculated from an energy-density-functional pseudopotential. At these radii the metallic energy is a minimum. Also tabulated are results from the all-electron calculation of Moruzzi *et al.* (Ref. 18) and experimental values from Wyckoff (Ref. 38). The radii are in a.u. (1 a.u. = 0.529 Å)

Metal	Experiment	Theory all-electron	EDFP
Li	3.25	3.17	3.63
Na	3.93	3.79	3.84
K	4.86	4.65	4.66
Rb	5.20	5.03	4.97
Cs	5.63		5.54
Mg	3.35	3.29	3.54
Ca	4.12	3.91	4.42
Al	2.99	2.97	3.26
Accuracy		3.0%	5.6%

TABLE VI. Bulk moduli as determined from an energy-density-functional pseudopotential calculations (Eq. 13). We also present experimental room-temperature bulk moduli from Gscheidner (Ref. 39). The all-electron values are from the work of Moruzzi *et al.* (Ref. 18). The bulk moduli are in dyn/cm^2 ($\times 10^{12}$).

Metal	Experiment	Theory all-electron	EDFP
Li	0.116	0.15	0.10
Na	0.068	0.09	0.072
K	0.032	0.04	0.047
Rb	0.031	0.03	0.040
Cs	0.020		0.023
Mg	0.354	0.41	0.33
Ca	0.152	0.17	0.13
Al	0.722	0.80	0.65
Accuracy		19.2%	17.6%

portance of d-state admixtures in the heavy alkali earths has recently been emphasized by Moriarty.[28]

In Table V we compile our computed equilibrium sphere radius R_s^0 for each metal and compare our calculation to experiment and to the work of Moruzzi *et al.*[18] Overall, in both calculations, the computed Wigner-Seitz sphere size appears to be relatively more accurate than does the cohesive energy. This is a strange result as one might expect the energies to be more accurate than volume sensitive quantities such as the radii. This may be an "atomic" problem since the radii depend solely on the metallic calculation. We speculate that the problem with the energies versus the radii may reside in the local-density approximation for exchange and correlation since the trend is similar in both calculations. Another interesting trend is that the all-electron calculation underestimates the sphere size in every case. This is not the situation for the present work; here all the monovalent metals (except Li) have smaller calculated R_s^0 than experiment, while all the polyvalent metals have larger R_s^0 than experiment. This suggests that the orbital hybridization effects associated with band splittings and at Brillouin-zone faces in Li and the polyvalent elements produce significant compressive forces which are omitted from our model. We believe that the present calculations are the first ones to isolate and quantify this effect of "incipient covalent bonding." The effect is large (~10%) and may be important in explaining, e.g., anomalies in the composition dependence of (c/a) ratios of Mg alloys[40] and vibrational anomalies in high-T_c superconductors.[41,42]

In Table VI we present our calculated bulk moduli for the simple metals which we have examined.

TABLE VII. Metallic pseudocharge-density parameters in a.u. [Eq. (9)]. These parameters will minimize the total energy of Eq. (1) for the equilibrium radius, in Ry, given in Table V.

Metal	b_1	b_2	c_1	c_2
Li	0.005 34	0.002 65	−0.048 7	−0.0570
Na	0.004 57	0.002 28	−0.066 8	−0.0317
K	0.002 83	0.001 36	−0.087 0	−0.0939
Rb	0.002 28	0.001 11	−0.085 7	−0.0867
Cs	0.001 63	0.000 830	−0.085 7	−0.0690
Mg	0.010 2	0.007 94	−0.020 7	−0.0312
Ca	0.005 61	0.003 71	−0.059 4	−0.0399
Al	0.017 1	0.014 6	0.004 47	0.0955

In terms of our spherical geometry the bulk modulus may be expressed as

$$B = 7.81(10^{12})\frac{1}{R_s^0}\left(\frac{\partial^2 E}{\partial R_s^2}\right)_{R_s^0}, \tag{13}$$

where B is in dyn/cm^2 and (E, R_s^0) are in atomic units. We evaluate the required second derivative by fitting a parabolic curve to the E vs R_s behavior. We also list the experimental values for the bulk moduli in Table VI and the results of the Moruzzi *et al.*[18] calculation. We do not distinguish between the room-temperature bulk modulus and the one appropriate at absolute zero (which should correspond to our calculations). First, our calculated bulk moduli are accurate to only ~20%, and second, the measured bulk moduli often have uncertainties comparable to the differences in the temperature change. Overall the agreement between our calculated values and experiment is quite good. This is especially true considering the computational and experimental difficulties. We note our calculated bulk moduli appear to be slightly superior to the all-electron calculated values. However, with the uncertainties involved, we do not view the small difference in accuracy as significant.

In Table VII we tabulate the charge-density parameters for the metal which minimizes the energy in Eq. (1). As with the atomic-density expression we use, there is some "overcompleteness" in our charge-density expression so we do not interpret in physical terms the behavior of the parameters. Rather we shall concentrate on examining the charge-density and energy-density trends in Na, Mg, and Al. In Fig. 5, we display the charge density for both the atom and the metal. Our results for Na are not surprising; they correspond quite closely to the results observed in the classic calculation of Wigner and Seitz.[35] For example, the density outside the core region is fairly constant. This is consistent with the Wigner-Seitz observation that the density is constant

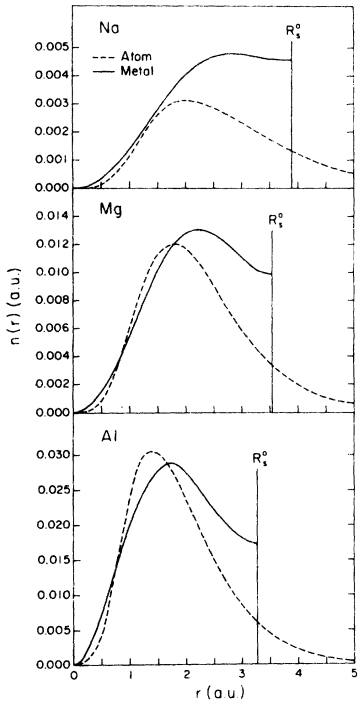

FIG. 5. Metallic and atomic pseudocharge densities for Na, Mg, and Al. Wigner-Seitz boundary conditions are employed for the metallic density. The derivative of the metallic density must vanish at the spherical boundary $r=R_s^0$.

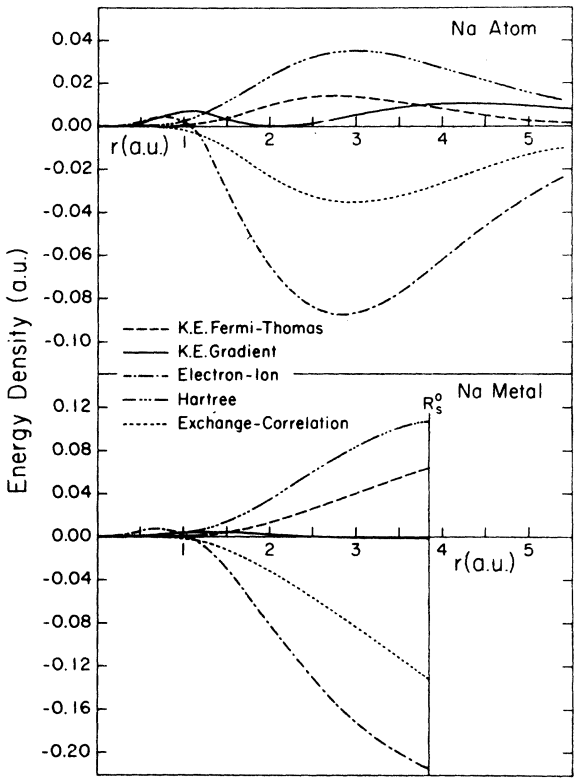

FIG. 6. Various energy contributions to the energy-density functional [Eq. (1)] for Na atom and metal plotted as a function of distance. R_s^0 is the metallic spherical radius. We include the phase factor of $4\pi r^2$ on the densities so that the area under each curve gives the total energy contribution.

over nearly 90% of the cell volume. We do note, however, that the density does not monotonically rise to the cell boundary but peaks at $r \simeq 2.6$ a.u. Again this is consistent with the Wigner-Seitz calculation. The existence of this peak arises from the electron-ion interaction and indicates the reduction in kinetic energy with constant density is slightly offset by the lowering of the potential energy through localizing charge near the ion-electron potential minimum. Mg and Al appear to mimic Na except that the density is more localized in both the metal and atom. Moreover, the relative change from atom to metal in the charge-density profile is not as dramatic in Al and Mg as compared to Na. This is to be expected. With increasing nuclear charge, the electron-ion potential becomes stronger and the effect of the cellular boundary conditions of the metal are lessened; away from the cell boundary, the atomic density remains relatively intact as we pass from the atom to the metal.

One advantage of the present analysis over other techniques is that we are able to examine in a straightforward fashion the real-space contributions of the various energy contributions to cohesion. We illustrate this for Na, Mg, and Al in Figs. 6–8. In these figures we have plotted the individual components of the energy-density functional for both the atom and the metal. We have included the $4\pi r^2$ volume factor in these plots so that the net area under each curve gives the total energy contribution.

The most striking aspect of Figs. 6–8 is the smallness of the kinetic energy correction term for the metallic densities. On the scale of the other energy contributions this term almost vanishes. Thus, we find that a local-kinetic-energy expression with only a gradient correction can be quite accurate for simple metals. While the correction is small for the metal, it is not small for the atom. In fact, for the Na atom the gradient term is comparable to the Thomas-Fermi term. This reinforces our arguments for fixing C_1 to atomic properties, where the gradient term is crucial in obtaining an accurate kinetic energy rather than by fixing C_1 to metallic properties where the gradient term is small.

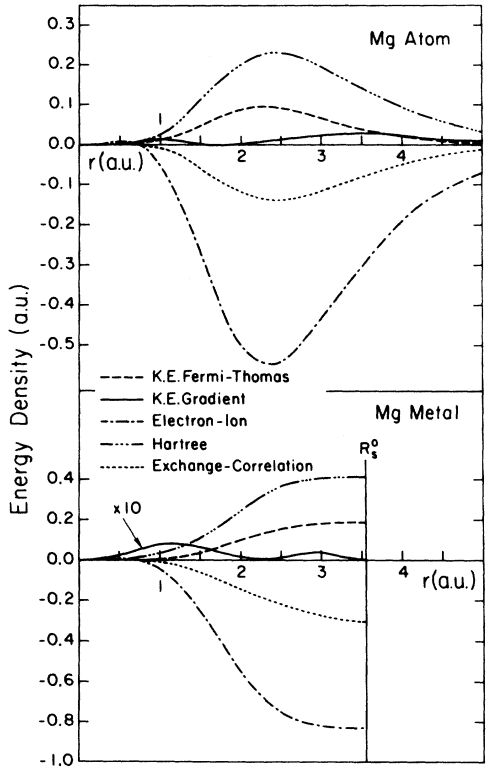

FIG. 7. Various energy contributions to the energy-density functional [Eq. (1)] for the Mg atom and metal. Note that the gradient-kinetic-energy term is so small for the metal it has been rescaled by a factor of 10 (see text).

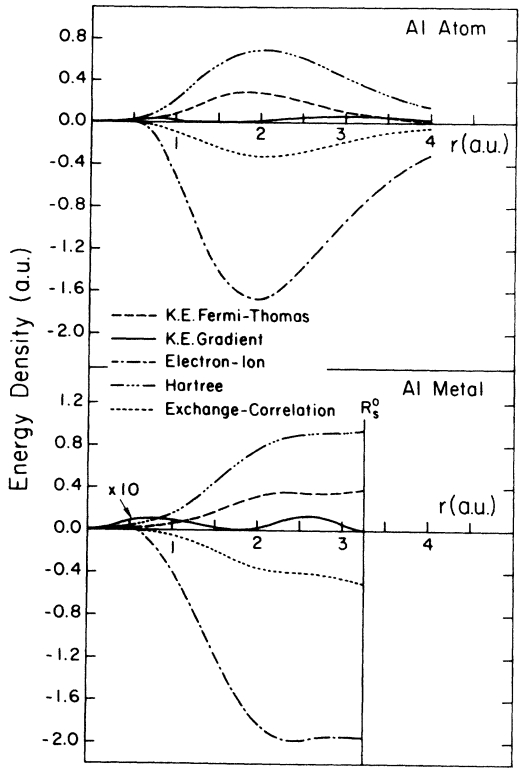

FIG. 8. Various energy contributions to the energy-density functional [Eq. (1)] for the Al atom and metal. The gradient-kinetic-energy term has been rescaled by a factor of 10.

Our calculated trends in the various energy components of the total energy appear compatible with the usual explanations of cohesion in metals. For example, in a "renormalized-atom" picture[21] the valence orbitals of the atom are terminated at the Wigner-Seitz radius and are renormalized. The renormalization increases the kinetic energy, but by "virial-theorem" arguments the potential energy is decreased by more than the kinetic energy increase. The resulting change lowers the energy of the renormalized atom and results in the metallic state being more stable than the atomic state. For the case at hand we might not expect a virial theorem argument to be valid. For example, our local-kinetic-energy operator may not reproduce the trends expected for a quantum-mechanical kinetic energy operator. Nevertheless, our results do appear to agree with the renormalized atom arguments. Namely, our potential-energy components decrease in energy in passing from the atom to the metal more than the kinetic energy increases.

Besides trends in the total kinetic energy and total potential energy, we note that the observed decrease of the gradient-kinetic-energy term in passing from the atom to the metal correlates quite well with the observed cohesive energy. This finding is in accord with the pioneering cohesion work of Wigner and Seitz.[35] Wigner and Seitz emphasize the role of phase matching of the wave functions at the cell boundary of a metal and the reduction of the curvature of the metallic wave functions as contrasted to the atomic case. Here we note the reduction of charge-density fluctuations as reflected by the gradient-kinetic-energy term (Figs. 6–8) appears to play a significant role in determining the cohesive energies. If the gradient term were removed from consideration, then we would find no cohesion: the sum of the homogeneous kinetic energy and potential energy is almost identical for the atom and metal. This is not surprising in view of previous discussions concerning the Fermi-Thomas approach with no inhomogeneity corrections.[6–8]

If the main source of cohesion in simple metals arises from a lowering of the total energy brought

about by new boundary conditions on the charge density, then the chief source of cohesion should be localized in real space at or near the metallic cell boundary. Recent work by Miedema and collaborators[19] on intermetallic alloys seems to suggest that cohesion arises in real space from changes in the elemental charge-density profile near the cell boundary.

With our formalism it is easy for us to examine the localization of cohesive energy contributions in real space. In order to demonstrate any localization graphically, we perform our spacial integrations about the cellular boundary; i.e., we choose to write:

$$E_m^0 = \int_0^{R_s^0} E_m(R_s^0 - r_c)\,dr_c, \tag{14}$$

$$E_a^0 = \int_0^{\infty} [E_a(R_s^0 - r_c) + E_a(R_s^0 + r_c)]\,dr_c, \tag{15}$$

and

$$E_c^0 = \int_0^{\infty} E_c(r_c)\,dr_c$$

$$= \int_0^{\infty} [E_m(R_s^0 - r_c) - E_a(R_s^0 - r_s) - E_a(R_s^0 + r_c)]\,dr_c, \tag{16}$$

where E_m is the metallic energy density, E_a is the atomic energy density, and E_c is the cohesive energy density. In Fig. 9 we display E_m, E_a, and E_c vs r_c. Since we have included the $4\pi r^2$ volume factor, the area under the curves give us the metallic energy (E_m^0), the atomic energy (E_a^0), and the cohesive energy (E_c^0), respectively. If all the cohesive energy origininated at the cell boundary, then we would have a strongly peaked structure for $E_c(r_c)$ with the maximum contribution occurring at the cell boundary ($r_c = 0$). In fact, we see all the negative cohesive energy contributions are strongly localized within approximately 1 a.u. of the cell boundary. We note there is some positive cohesive-energy contribution in Al. This contribution peaks at about 1.5 a.u. from the cell boundary, and it arises from a "rigid" shift in the charge density of the atom in passing to the metal. (See Fig. 5.) We emphasize that this is not a negative contribution to the cohesive energy and that the binding contributions are strongly localized at the cell boundary.

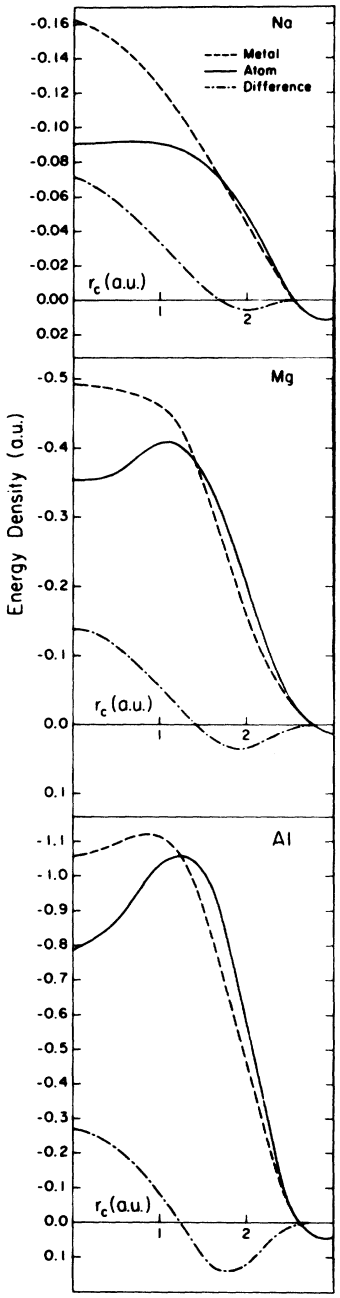

FIG. 9. Real-space energy-density contributions to the cohesive energy of Na, Mg, and Al. $r_c = 0$ corresponds to the cell boundary. The atomic, metallic, and difference curves correspond to the definitions in Eqs. (15) and (16). The area under each curve gives the atomic E_a^0, metallic E_m^0, and cohesive energies E_c^0, respectively. Note the strong localization of the cohesive-energy contributions at the cell boundary. (Also see text.)

VI. CONCLUSIONS

Since we listed in our introductory comments some of the deficiencies of Thomas-Fermi approaches, it would seem appropriate in summary to emphasize the positive aspects of our study. By combining a local-density expression for the kinetic energy and a hard-core pseudopotential for the electron-ion interaction energy we were able to examine several simple metals in an accurate,

yet convenient, fashion. We did not need to calculate any band-structure properties nor individually match wave-function phases. By considering only charge densities, we were able to account quantitatively for all the static properties of the metals. We stress this aspect because phase matching has been emphasized so often in discussions of metallic cohesion in metals.[43] Our studies indicate this is not a correct viewpoint, at least for simple metals.

The only real deficiency of the present study is its neglect of nonlocal effects both in the pseudopotential (which should be l dependent) and the kinetic energy (orbital hybridization). Nonlocal effects would certinaly be important in any study of transition metals or noble metals. In fact, as we have discovered in our study of Li and Ca, nonlocal effects may be important in what are nominally simple metals. (Some preliminary calculations we have performed on Ga indicate the neglect of nonlocal effects may introduce an error nearly twice as large as that found for Al.) We feel from the present studies that it should be possible to modify the pseudopotential to include nonlocal or l-dependent effects, and we hope to address this question in a subsequent paper.

Finally, while we have been able to analyze in some detail several simple metals in a unique fashion, we feel the study of metals per se is not the strength of this method. First, studies for most elemental metals already exist in the literature in the form of all electron calculations, e.g., Moruzzi *et al.*[18] Second, our calculations contain one nonderivable parameter for the gradient expansion term of the kinetic energy. The existence of this parameter certainly restricts our method as an *ab initio* means of studying metallic properties. On the positive side, our method may prove to be a very powerful technique for studying alloy formation. In particular, our approach clearly resembles the intermetallic alloy model of Miedema and collaborators.[19] However, unlike Miedema's semiempirical scheme, our approach has a definitive microscopic interpretation which we have shown here parallels quite closely the results of the best *ab initio* elemental studies.

ACKNOWLEDGMENT

The author would like to thank Dr. J. C. Phillips for a critical reading of the manuscript.

[1]A review of the Thomas-Fermi approximation is given by N. H. March, Adv. Phys. 6, 1 (1957).
[2]P. Hohenberg and W. Kohn, Phys. Rev. 136, B863 (1964).
[3]W. Kohn and L. J. Sham, Phys. Rev. 140, A113 (1965).
[4]L. J. Sham and W. Kohn, Phys. Rev. 145, 651 (1966).
[5]It is possible to reproduce the shell structure of the atom with an EDF approach if suitable constraints are imposed on the charge density. See W. P. Wang and R. G. Parr, Phys. Rev. A 16, 891 (1977).
[6]E. Teller, Rev. Mod. Phys. 34, 627 (1962). This paper presents arguments that Thomas-Fermi-Dirac methods cannot yield stable, i.e., bound, solutions for molecules. However, here we go beyond the Thomas-Fermi-Dirac method by including gradient corrections to the kinetic energy term.
[7]N. L. Balazs, Phys. Rev. 156, 42 (1967).
[8]J. W. Sheldon, Phys. Rev. 99, 1291 (1955).
[9]G. L. Oliver and J. P. Perdew, Phys. Rev. A (to be published).
[10]W. P. Wang, R. A. Parr, D. R. Murphy, and G. A. Henderson, Chem. Phys. Lett. 43, 409 (1976).
[11]J. A. Alonso and L. Girifalco, Phys. Rev. B 17, 3735 (1978).
[12]Y. Tal and R. F. W. Bader, Int. J. Quantum Chem. 12, 153 (1978).
[13]J. R. Chelikowsky and J. C. Phillips, Phys. Rev. B 18, 2453 (1978); W. Andreoni, A. Baldereschi, E. Biémont, and J. C. Phillips, Phys. Rev. B 20, 4814 (1979); J. St. John and A. Bloch, Phys. Rev. Lett. 33, 1075 (1974); A. Zunger and M. L. Cohen, Phys. Rev. Lett. 41, 53 (1978), and references therein.
[14]D. R. Hamann, Phys. Rev. Lett. 42, 662 (1979).
[15]A. Meyer, I. K. Umar, and W. H. Young, Phys. Rev. B 4, 2287 (1971), These authors have employed a local energy functional with pseudopotentials. However, the pseudopotentials were not constructed within the EDF framework, and the resulting pseudodensities are in poor agreement with fully quantum-mechanical calculations.
[16]B. Y. Tong, Phys. Rev. B 6, 1189 (1972).
[17]J. F. Janak, V. L. Moruzzi, and A. R. Williams, Phys. Rev. B 12, 1257 (1975).
[18]V. L. Moruzzi, J. F. Janak, and A. R. Williams, *Calculated Electronic Properties of Metals* (Pergamon, Elmsford, N.Y., 1978).
[19]A. R. Miedema, R. Boom, and F. R. de Boer, J. Less-Common Met. 4, 283 (1975); R. Boom, F. R. de Boer, and A. R. Miedema, *ibid.* 45, 237 (1976); 46, 271 (1977), and references therein.
[20]J. A. Alonso and L. A. Girifalco, J. Phys. Chem. Solids 39, 79 (1978), and references therein.
[21]L. Hodges, R. E. Watson, and H. Ehrenreich, Phys. Rev. B 5, 3953 (1972).
[22]E. S. Machlin, Acta Metall. 22, 109 (1974).
[23]D. G. Pettifor, J. Phys. F 7, 613 (1977); 8, 219 (1978); Commun. Phys. 1, 141 (1976).
[24]V. K. Ratti and J. M. Ziman, J. Phys. F 4, 1684 (1974).
[25]C. Hodges, J. Phys. F 7, L247 (1977).
[26]G. D. Gelatt, Jr., H. Ehrenreich, and R. E. Watson, Phys. Rev. B 15, 613 (1977).
[27]O. Gunnarsson, B. I. Lundqvist and J. W. Wilkins, Phys. Rev. B 10, 1319 (1974).
[28]J. A. Moriarty, Phys. Rev. B 19, 609 (1979) and (un-

published). Also U. von Barth and G. D. Gelatt (unpublished).
[29]G. F. Von Weizsacker, Z. Phys. 96, 431 (1935).
[30]D. A. Kirzhnitz, Zh. Eksp. Teor. Fiz. 32, 115 (1957) [Soviet Phys.-JETP 5, 64 (1957)].
[31]V. Heine, Solid State Phys. 24, 1 (1970); M. L. Cohen and V. Heine, *ibid.* 24, 37 (1970); V. Heine and D. Weaire, *ibid.* 24, 239 (1970).
[32]K. Schwarz, Phys. Rev. B 5, 2466 (1972).
[33]We solved for the one-electron wave functions and eigenvalues as outlined in F. Herman and S. Skillman, *Atomic Structure Calculations* (Prentice-Hall, Englewood Cliffs, N.J., 1963).
[34]O. Gunnarsson, B. I. Lundqvist, and S. Lundqvist, Solid State Commun. 11, 149 (1972).
[35]E. P. Wigner and F. Seitz, Phys. Rev. 43, 804 (1933); 46, 509 (1934).
[36]*Handbook of Chemistry and Physics*, 56th ed. (Chemical Rubber, Cleveland, Ohio, 1975).
[37]G. N. Lewis, M. Randall, K. S. Pitzer, and L. Brewer, *Thermodynamics*, 2nd ed. (McGraw-Hill, New York, 1961).
[38]R. W. G. Wyckoff, *Crystal Structure*, 2nd ed. (Interscience, New York, 1963).
[39]K. Gschneidner, Jr., Solid State Phys. 16, 275 (1964), and references therein.
[40]W. Pearson, *The Crystal and Physics of Metals and Alloys* (Wiley, New York, 1972).
[41]J. C. Phillips, Phys. Status Solidi B 77, 259 (1976).
[42]C. Varma and W. Weber, Phys. Rev. B 19, 6143 (1979), and references therein.
[43]E. Wigner and F. Seitz, Solid State Phys. 1, 97 (1955).